JOURNAL OF Materials CHEMISTRY

One-dimensional nanostructures of trigonal tellurium with various morphologies can be synthesized using a solution-phase approach

Brian Mayers and Younan Xia*

Department of Chemistry, University of Washington, Seattle, Washington 98195, USA.
E-mail: xia@chem.washington.edu

Received 29th January 2002, Accepted 14th March 2002
First published as an Advance Article on the web 19th April 2002

This article describes a solution-phase, self-seeding approach to the large-scale synthesis of one-dimensional (1D) nanostructures of trigonal tellurium (*t*-Te) with diameters ranging from 50 to hundreds of nanometers, and lengths up to tens of micrometers. These highly anisotropic nanostructures were formed through the reduction of orthotelluric acid (or tellurium dioxide) by hydrazine at various refluxing temperatures. Nuclei formed in the reduction process had a strong tendency to grow along the *c*-axis due to the inherently anisotropic structure of *t*-Te. Depending on the solvent and refluxing temperature, the growth of *t*-Te nanostructures was found to follow two distinct paths. When the reaction was refluxed in water and at temperatures below 100 °C, the initial reduction products were a mixture of nanocrystallites of *t*-Te and spherical colloids of amorphous tellurium (*a*-Te). When this mixture was aged at room temperature, the *a*-Te colloids slowly dissolved into the solution and grew into nanowires on the nanocrystallites of *t*-Te. When the reaction was carried out in pure ethylene glycol (or mixtures with water) and refluxed at temperatures above 100 °C, the 1D nanostructures of *t*-Te were directly formed in the reduction process. The exact morphology of these anisotropic nanostructures was mainly controlled by the refluxing temperature (T_r); typical examples include spines ($T_r < 100$ °C), filaments ($T_r = 100$–160 °C), needles ($T_r = 160$–180 °C), and tubular structures ($T_r > 180$ °C). These uniform, relatively monodispersed 1D nanostructures could form stable dispersions in ethylene glycol or water, and be used as the building blocks or templates to generate more complex nanostructured materials.

I. Introduction

Nanostructures and nanomaterials have been the subject of intensive research for their potential applications in electronics, photonics, and catalysis.[1] They are also ideal candidates for investigations on the dependence of optical, electrical, magnetic, and mechanical properties on size confinement.[2] One of the primary hurdles in this field has been to produce nanostructures with well-controlled morphologies and dimensions without the necessity for costly and complex processing. Although a number of advanced nanolithographic methods (including electron-beam writing and deep UV photolithography) can generate well-defined nanostructures as small as a few nm,[3] the development of these techniques for high-volume production will require dedicated machinery and can be prohibitively expensive. Chemical methods (the so-called bottom up approach) may provide a more promising route to nanostructures (or nanomaterials) in terms of throughput, cost, and the potential for large-scale production.[4] Unfortunately, chemical methods are often limited in morphological control due to their tendency to form zero-dimensional (0D) nanostructures such as nanocrystallites or spherical colloids.[5] Physical templates — for example, channels in porous materials or structures self-assembled from surfactants — are usually required to generate nanostructures with other complex morphologies.[6] Although the use of a physical template allows for good morphological and dimensional control over the nanostructures, such a method is intrinsically limited in terms of production scale and nanostructure throughput.

A number of chemical methods have recently been demonstrated or re-examined for making one-dimensional (1D) nanostructures without the use of any physical template. Most of these methods are based on vapor–solid (VS) and vapor–liquid–solid (VLS) mechanisms,[7] in which dual-functional metal nanocrystallites are often used both as nuclei and as a means to confine and direct the growth of the 1D nanostructures. Examples of 1D nanostructures that have been successfully prepared using these methods include carbon nanotubes,[8] metal and semiconductor nanowires,[9] and a variety of inorganic nanowhiskers.[10] More recently, solution-phase procedures have also been demonstrated for generating nanowires of silicon and III–V semiconductors.[11] Solution-phase reactions have the additional advantage that seeds are not restricted to a two-dimensional (2D) growth plane, and copious quantities of well-defined nanostructures can be obtained with relative ease compared to methods based on vapor-phase reactions. Our group has been actively exploring new chemical approaches to 1D nanostructures. Specifically, we are focusing on templateless, solution-phase routes. In order to avoid the necessity of heterogeneous seeds, physical templates, or surfactants, we have concentrated on semiconducting materials that have a natural tendency for 1D anisotropic growth.

Trigonal tellurium (*t*-Te), as shown in Fig. 1A, has a highly anisotropic crystal structure consisting of helical chains of covalently bound atoms, which are in turn bound together through van der Waals interactions into a hexagonal lattice.[12] This structure gives *t*-Te inherent chirality, as well as a strong tendency toward 1D growth. A *p*-type semiconductor ($\sigma \approx 5$ S cm^{-1}), trigonal tellurium also exhibits a unique combination of many other useful and interesting properties: for example, photoconductivity; catalytic activity toward hydration or oxidation reactions; and high piezoelectric, thermoelectric, or nonlinear optical responses.[13] In addition, solid tellurium reacts readily with other elements to generate a wealth of functional materials such as Bi_2Te_3, ZnTe, and CdTe.[14] As we have already demonstrated, trigonal selenium (which has a crystal structure nearly identical to *t*-Te) could be readily grown into uniform nanowires from the solution phase. The diameters of these single crystalline nanowires could also be

DOI: 10.1039/b201058e

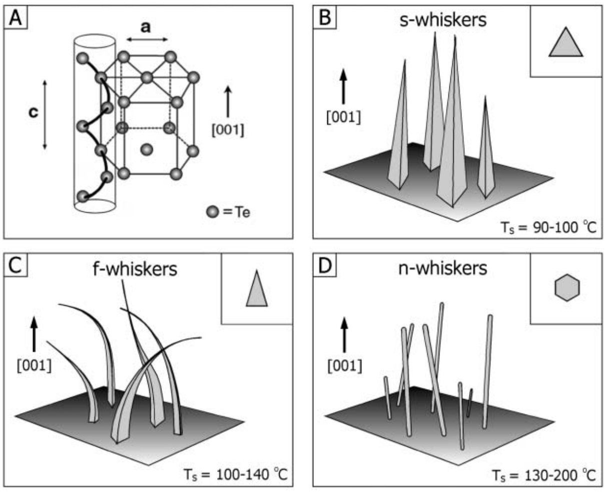

Fig. 1 (A) The crystal structure of *t*-Te is highly anisotropic, with the basic unit being helical chains of covalently bound tellurium atoms. These chains are held together to form a hexagonal lattice *via* weaker van der Waals forces. Such an inherently anisotropic structure tends to grow along the [001] direction even in an isotropic medium. Depending on the substrate temperature (T_s), *t*-Te crystals grown from the vapor phase were shown to exhibit a number of different morphologies: (B) triangular, spine-shaped whiskers at T_s = 90–100 °C; (C) filamentary, blade-shaped whiskers when Ts was raised to 100–140 °C; and (D) needle-like whiskers when T_s was controlled in the range of 130–200 °C. The inset of each plate indicates the cross-section of that particular type of whisker.

easily changed from ~10 nm to several hundred nanometers by controlling the experimental conditions.[15] In the present work, we describe the synthesis of 1D nanostructures of *t*-Te with well-controlled morphologies using a self-seeding, solution-based approach.

II. Experimental procedures

Materials

Orthotelluric acid (H_6TeO_6, 99.99%), tellurium dioxide (TeO_2, 99.995%) and hydrazine monohydrate ($N_2H_4H_2O$, 98%) were purchased from Aldrich (Milwaukee, WI). They were prepared as stock solutions by diluting with 18 MΩ water (E-Pure, Dubuque, IA), or by diluting with anhydrous ethylene glycol (EG, HOC_2H_4OH, 99.8% Aldrich). All chemicals were used without further purification. Polished silicon (100) wafers (test grad, phosphorous-doped) were obtained from Silicon Sense (Nashua, NH). Pre-cleaned glass slides (Micro slides #2947) were purchased from Corning Glass (Corning, NY).

Preparation of tellurium nanostructures

The *t*-Te nanostructures were prepared in three different solvent systems that include water, EG, and water–EG mixtures. Orthotelluric acid was reduced by hydrazine in these solvents refluxed at temperatures in the range of 20–200 °C. Tellurium dioxide was directly reduced by EG heated to 180 °C. In general, the reactions were stirred and heated until the initial reduction was completed (~10 min). Reaction mixtures were then air cooled, covered, and allowed to age in the dark at room temperature. Samples were taken periodically for electron microscopy characterization. Depending on the solvent and the range of refluxing temperatures, the growth of *t*-Te nanostructures was found to follow two distinct paths. When the reaction was refluxed in water and at temperatures below 100 °C, the initial reduction products were a mixture of nanocrystallites of *t*-Te and spherical colloids of amorphous tellurium (*a*-Te). When this mixture was cooled and aged at room temperature, the *a*-Te colloids slowly dissolved into the solution and grew into nanowires on the seeds of *t*-Te nanocrystallites. When the reaction was performed in pure ethylene glycol (or a mixture with water) that was refluxed at temperatures above 100 °C, the 1D nanostructures of *t*-Te were directly formed in the reduction process. No additional aging process was necessary. The detailed procedures for three different solvent systems are described bellow. Reactions were typically performed on the tens of milligrams scale, but were readily scaled up to the gram scale with no change in the products. In all cases, the mass yield of the reaction was nearly quantitative since all of the starting material was reduced to pure tellurium.

(*i*) Pure water: orthotelluric acid was added to 10 mL water in a round bottom flask to give an 8 mM solution. This flask was then placed in an oil bath for temperature regulation (in the range from 20 to 100 °C), fitted with a condenser, and stirred magnetically. A hydrazine solution (1×10^{-2} moles in 1 mL of 18 MΩ pure water) was rapidly added to the orthotelluric acid solution under constant magnetic stirring.

(*ii*) Pure ethylene glycol: orthotelluric acid was added to 10 mL of anhydrous EG and heated to 80 °C in a round bottom flask until the precursor was completely dissolved (in a few min) to give an 8 mM solution. This flask was then placed in an oil bath for temperature regulation (in the range from 100 to 200 °C), fitted with a condenser, and stirred magnetically. A hydrazine solution (1×10^{-2} moles in 1 mL EG) was rapidly added under constant magnetic stirring. Alternatively, tellurium dioxide was added to 10 mL of anhydrous EG in a round bottom flask to give an 8 mM solution. This flask was equipped with a condenser and magnetic stir-bar, and heated in an oil bath to 180 °C. Tellurium dioxide was readily reduced by EG at this temperature and no further addition of hydrazine was required.

(*iii*) Mixtures of ethylene glycol and pure water: orthotelluric acid was added to 10 mL of anhydrous EG and 1 mL of 18 MΩ pure water to give an 8 mM solution. The container was then placed in an oil bath, and stirred magnetically. The solution was heated to reflux (140 °C) and allowed to boil off water without a condenser at an increase in temperature by $\sim 2\ ^\circ C\ min^{-1}$. When the desired temperature was reached, a hydrazine solution (1×10^{-2} moles in 1 mL EG) was rapidly added under constant magnetic stirring.

Instrumentation

Scanning electron microscopy (SEM) images were obtained using a field emission microscope (FSEM, JEOL-6300F, Peabody, MA) or an environmental microscope (ESEM, Phillips, Electroscan-2020, Wilmington, MA). The FSEM was operated with an accelerating voltage of 15 kV, and the ESEM was operated with an accelerating voltage of 20–30 kV and a chamber pressure of 5 Torr. All SEM samples were prepared by putting drops of diluted (by ~10 times) reaction mixtures on silicon substrates, and allowing the solvent(s) to evaporate slowly at room temperature in fume hoods. Transmission electron microscopy (TEM) images and electron microdiffraction patterns were obtained using a JEOL-1200EX-II electron microscope (Peabody, MA) with an accelerating voltage of 80 kV. Samples for TEM were prepared by placing drops of diluted (by ~20 times) solutions on Formvar-coated, copper TEM grids (Ted Pella, Redding, CA). For X-ray diffraction (XRD) studies, large quantities of nanostructures were obtained by filtration of concentrated dispersions through polycarbonate membranes (Nucleopore®, #110408, Corning, MI). The powders retained on the membranes were transferred onto glass substrates, and XRD measurements were then acquired using a Phillips PW1710 diffractometer with Cu K_α radiation ($\lambda = 0.15418$ nm).

III. Results and discussion

The morphologies of tellurium whiskers

Furuta and coworkers have extensively studied the morphologies of tellurium whiskers grown on the surfaces of solid substrates from the vapor phase.[16] When the substrate temperature (T_s) was increased from 90 to 200 °C, they observed a mixture or any one of the three basic morphologies shown in Figs. 1(C,D). At T_s = 90–100 °C, spine-shaped crystals (or s-whiskers) were observed having triangular cross-sections and tapered tips. When T_s = 100–140 °C, filamentary crystals (or f-whiskers) with elongated triangular cross-sections and long tapered tips were obtained. With T_s = 130–200 °C, needle-shaped crystals (or n-whiskers) having uniform cross-sections and high aspect ratios ($\sim$1000 : 1) were formed. The growth directions of all these crystals were parallel to the *c*-axis, as directed and confined by the inherently anisotropic structure of *t*-Te (Fig. 1A). At $T_s > 130$ °C, blade-shaped crystals with their primary growth directions running perpendicular to the *c*-axis were also found to coexist with crystals having other morphologies. We expected that tellurium nanostructures synthesized *via* solution-phase routes should exhibit a similar morphological transitions when the nucleation and growth temperature was raised from 20 to 200 °C. The major difference between solution- and vapor-based systems is that the tellurium atoms are solvated in the solution phase, and there might exist a difference in the diffusion rates of active species and thus growth kinetics.

Pure water as the solvent

The first system that we have studied involves the reduction of orthotelluric acid by hydrazine in pure water. In this case, hydrazine was added to an aqueous solution of orthotelluric acid, and tellurium atoms were formed according to the following redox reaction:[13]

$$2\ H_6TeO_6 + 3\ N_2H_4 \rightarrow 2\ Te\ (\downarrow) + 3\ N_2\ (\uparrow) + 12\ H_2O$$

The reduction was extremely rapid even at room temperature, and the reaction mixture quickly changed from clear to brown and finally to black within the first minute of reaction. Similar to the reduction of selenious acid by hydrazine,[15,17] the initial products were found to be spherical colloids (polydispersed in size, with an average diameter on the order of $\sim$1 μm) of *a*-Te and nanocrystallites ($\sim$50 nm in size) of *t*-Te. When this aqueous suspension containing a mixture of *a*-Te colloids and *t*-Te nanocrystallites was aged at room temperature, the spherical colloids of *a*-Te would slowly dissolve into the solution phase due to the relatively high free energy of *a*-Te as compared to *t*-Te. The tellurium dissolved from *a*-Te colloids could be subsequently deposited onto the surfaces of *t*-Te nanocrystallites (seeds) and grown into single crystalline nanowires. Such a solid–solution–solid transformation resembles the Ostwald ripening process that has been intensively studied in the context of a colloidal or emulsion system.[18] Over the course of several hours, some of the amorphous colloids were converted into spine-shaped nanowires with relatively high aspect-ratios (typically $\sim$80 : 1), giving the black solution a precipitate of silvery tint. In this case, the 1D morphology of the final product was determined by the highly anisotropic characteristics of the building blocks – that is, the linearity of infinite, helical chains of Te atoms contained in the trigonal phase of solid tellurium.

Figs. 2A and 2B show SEM images of some characteristic nanowires of *t*-Te that were formed by reducing orthotelluric acid with hydrazine in water at $\sim$20 °C, followed by aging at room temperature for a period of two weeks. Some amorphous tellurium was still present in this sample; it eventually disappeared over a period of several months. The shape of these nanowires is similar to that of s-whiskers observed by Furuta *et al.* in the vapor-phase synthesis.[16] Each wire is characterized by equilateral triangular cross-sections whose dimensions continuously change from $\sim$10 nm at tips to $\sim$50 nm in the middle. The lengths of these nanowires could vary from 500 nm to several micrometers. The relatively uniform distribution in lateral dimension could be attributed to the fact that the formation of nanocrystalline seeds was an instantaneous process (the nucleation event likely occurred over a very short period of time). Growth could occur over a much longer period (from weeks to months) until all *a*-Te colloids had disappeared from the solution. These nanowires aggregated into an interpenetrated network that settled to the bottom of the reaction container over the course of several days. Such an aggregation could be avoided by decreasing the initial concentrations of reactants and by adding some surfactants — such as poly(vinyl pyrrolidone) (PVP) or alkanethiols — to keep the nanowires well-dispersed in the solution phase.

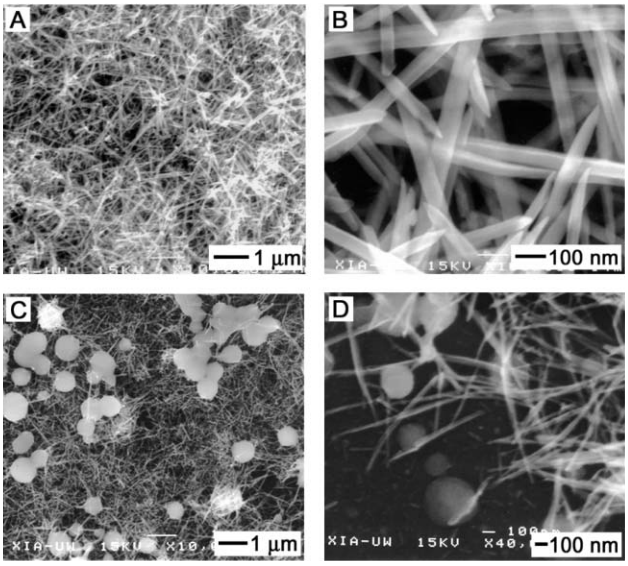

Fig. 2 (A) Low and (B) high magnification SEM images of *t*-Te nanowires synthesized by reducing orthotelluric acid with hydrazine in water at ambient temperature ($\sim$20 °C). The shape of these nanowires was similar to that of s-whiskers having triangular cross-sections and tapered ends. (C, D) SEM images of *t*-Te nanowires synthesized using a similar procedure, except that the reduction reaction was carried our at $\sim$100 °C. These nanowires also displayed a morphology similar to that of s-whiskers. Note that this sample still contained *a*-Te colloids due to a relatively short period of aging time.

Reduction at elevated temperatures yielded results similar (Figs. 2C and 2D) to the room temperature reaction, except that the formation was more rapid. At $\sim$100 °C, for example, the reaction solution immediately turned black when the reducing agent was added, and a more vigorous reduction was observed. The final products were also spine-shaped nanowires, exhibiting a three-faced morphology. The initial concentration of orthotelluric acid did not affect the eventual morphology. Above a critical concentration ($\sim 10^{-2}$ mM) the products were always spine-like nanowires crystallized purely in the trigonal phase. The growth directions of all these nanowires were parallel to the *c*-axis of the crystal lattice. Below the critical concentration, only spherical colloids of *a*-Te were formed in the temperature range from 20 to 100 °C.

Pure ethylene glycol as the solvent

As a solvent, water is limited to a maximum reflux temperature of 100 °C at ambient pressure. In order to increase the range of temperatures for the reaction, pure EG (boiling point ≈ 197 °C) was employed as a solvent. Ethylene glycol has a similar chemical structure to that of water: hydroxy groups on opposite ends of an ethylene group.[19] However, since orthotelluric acid was not soluble in EG at room temperature, it was necessary to heat the EG to 80 °C before the acid precursor could be completely dissolved. The ability of EG to reduce some metal ions at elevated temperature was of initial concern because of the possibility of premature reduction of orthotelluric acid by the solvent itself before hydrazine was added.[20] Our recent study indicated that complete reduction of Te(VI) in the acid precursor to Te(0) by EG did not occur until the solution was heated to temperatures > 185 °C.[21] In this case, the acid precursor decomposed into TeO_2 (or other mixed valence species) that could be readily reduced to Te(0) by EG.

Reduction of orthotelluric acid by hydrazine at temperatures below ~ 100 °C yielded only colloids of *a*-Te, probably due to the high viscosity of the solvent, and thus poor transport of Te atoms and low probability to form nanocrystalline seeds of *t*-Te. Products of the same reduction reaction at higher temperatures (100–196 °C) were remarkably different from those obtained in aqueous solutions. In general, the products were similar to the f-whiskers generated by Furuta *et al.* in the vapor phase.[16] Fig. 3 shows the progression of *t*-Te nanostructures when the reaction temperature was increased from 100 to 180 °C. As the temperature was raised, the nanowires became longer but the morphology remained essentially unchanged. At all temperatures, these nanowires had a length between 2 and 10 μm, with a taper of 1.2 degrees. These results differ from what was observed for the vapor phase synthesis in that there was no morphological transition when the temperature was raised from 100 to 180 °C. Tellurium nanowires grown in the vapor phase underwent a transition from s- to f- and n-whiskers over this temperature range. As with the nanowires grown from the aqueous phase, their primary growth directions were all along the *c*-axis of the crystal lattice.

At 196 °C, a new morphology was observed (Figs. 3G and 3H) for the Te nanostructures. Reduction of orthotelluric acid by EG gave rise to hexagonal seeds as previously reported.[21] If the high temperature was maintained without addition of any reducing agent, these nuclei would grow into tubular structures with hollow interiors. In this case, the addition of hydrazine induced the growth of filamentary nanowires off alternating corners of the hexagonal seeds to form the specific morphology illustrated in Fig. 3H. The separation of nucleation and growth steps promoted a greater monodispersity in the final product, as well as a unique tri-tip morphology. These nanowhiskers had an average diameter of 220 nm and length of 3.9 μm. The lateral dimensions of these seeds were mainly determined by the initial concentration of orthotelluric acid, while the growth rate was highly dependent on the hydrazine concentration. These two parameters allowed for a direct control over both length and width of the tellurium nanostructures.

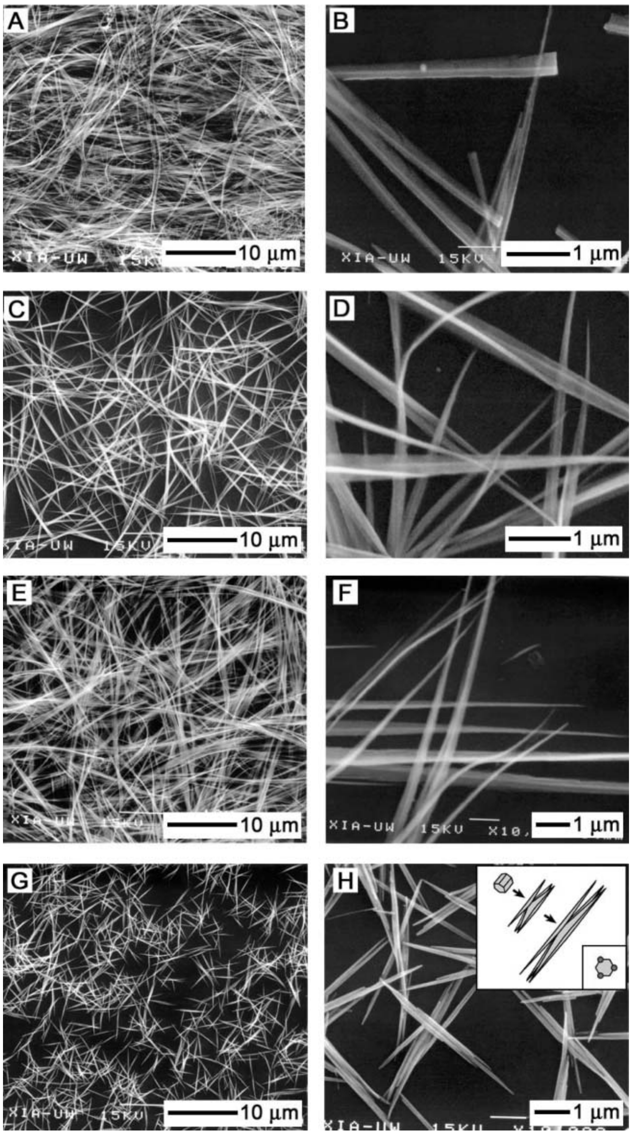

Fig. 3 Low and high magnification SEM images of *t*-Te nanowires synthesized by reducing orthotelluric acid with hydrazine in ethylene glycol refluxed at (A, B) 100 °C, (C, D) 140 °C, and (E, F) 180 °C. All these nanostructures had a distinct shape similar to that of f-whiskers, and this morphology changed very little with temperature. (G, H) When the refluxing temperature was increased to 196 °C, a remarkable change in morphology occurred. Reduction of telluric acid by the ethylene glycol yielded uniform hexagonal nuclei of *t*-Te. Subsequent addition of hydrazine induced the growth of filamentary nanowires at the edges of each seed giving a tri-tipped, tubular structure. The inset shows a schematic of the growth process from hexagonal seed to tri-tipped nanotube. The lower right corner of the inset shows a cross-sectional view of the nanotube.

Mixtures of water and ethylene glycol as the solvents

We were most interested in *t*-Te nanostructures with both controllable lengths and uniform cross sections. The solvent systems based on either pure EG or pure water did not provide this type of control. A combination of water and EG, however, has allowed for this through the formation of needle-like nanostructures. Water was initially added to pure EG as a means of temperature control. Fig. 4 shows the normal boiling points of water–EG mixtures.[19] By introducing various amounts of water into EG, the reflux temperature of the reaction mixture could be precisely controlled in the range of 100 to 197 °C. The morphology of Te nanostructures was found to be very sensitive to small changes in water percentage and refluxing temperature. Fig. 5 shows SEM images of *t*-Te nanostructures that were synthesized at three different solvent compositions. With 3% weight of water in EG (bp $\approx$ 166 °C), the resultant nanostructures had a morphology similar to that of products obtained when pure EG was used as the solvent. These nanostructures displayed a filamentary morphology with long tapering ends (Fig. 5A). When the weight percentage of water was slightly reduced to 2.4% (bp $\approx$ 170 °C), the blades of these nanowires seemed to flatten out with less of a taper, and a more uniform cross section (Fig. 5B). At 1.7% weight of water in EG (bp $\approx$ 176 °C), the Te nanostructures were completely converted into the needle-type morphology. These nanowires had characteristic rounded tips and uniform cross-sections (Fig. 5C).

By finely tuning the weight percentage of water in EG, it was also possible to control the lateral dimensions and uniformity of the *t*-Te nanostructures. Fig. 6 depicts another reduction reaction that was performed at 178 °C, with 1.5% weight of water in EG. The nanorods shown in this figure had an average length of 1.80 ± 0.16 μm, and width of 98 ± 3 nm. They were

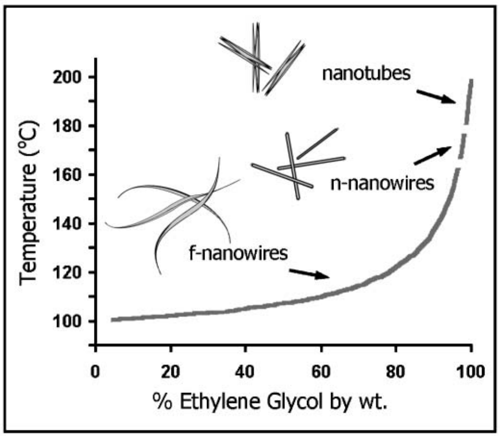

Fig. 4 The boiling points of ethylene glycol and water mixtures having different ratios. The general morphologies of Te nanostructures observed at different solvent compositions (and thus refluxing temperatures) were also indicated in this drawing. Needle-shaped nanowires were only formed in a very narrow range of temperature (174–182 °C). Below this temperature range, filamentary nanowires were generated. Above this temperature range, tubular nanostructures with tri-tipped whiskers were observed.

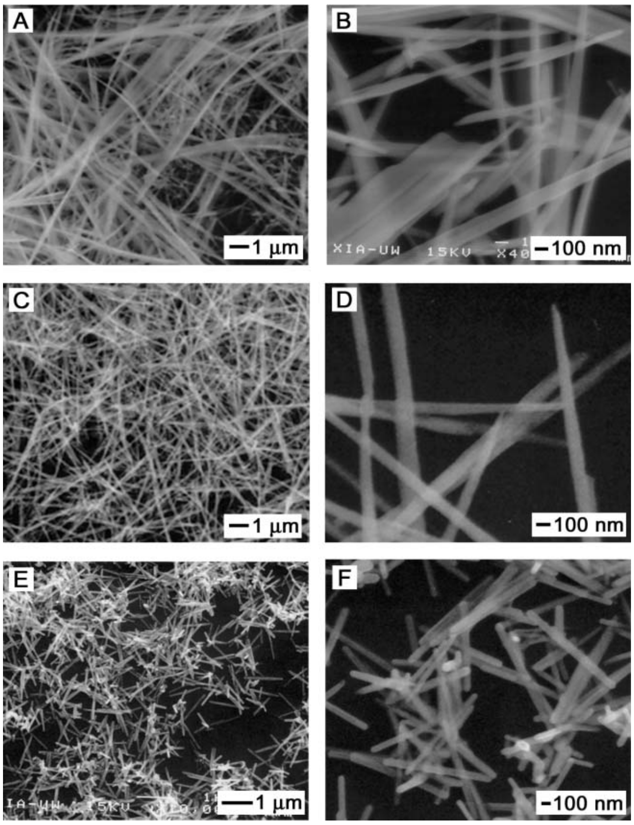

Fig. 5 (A) Low and (B) high magnification SEM images of tellurium filamentary nanowires synthesized by reducing orthotelluric acid with hydrazine in an ethylene glycol–water mixture boiling at 166 °C. The nanostructures produced from this system had a morphology similar to those formed in pure ethylene glycol at the same temperature. (C, D) SEM images of Te nanowires synthesized in an ethylene glycol–water solvent system boiling at 170 °C. The filamentary nanowires began to display rounded tips characteristic of n-whiskers. (E, F) SEM images of Te nanowires obtained from an ethylene glycol–water solvent system boiling at 176 °C. The nanowires had fully rounded tips and uniform cross sections along the longitudinal direction.

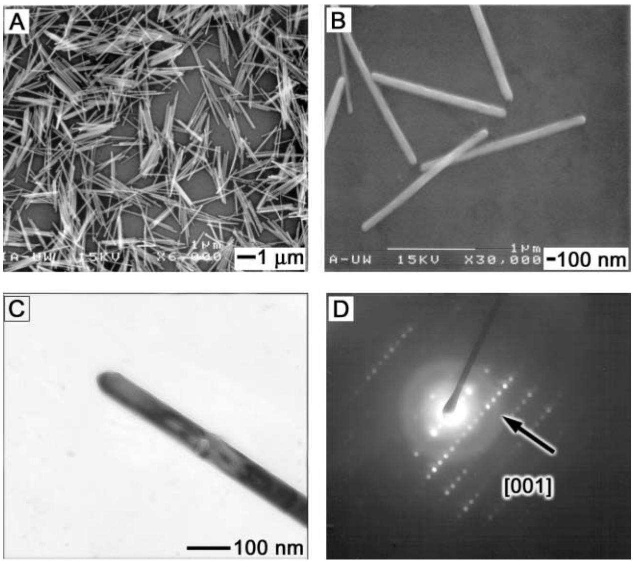

Fig. 6 (A) Low and (B) high magnification SEM images of tellurium n-nanowires formed by reducing orthotelluric acid with hydrazine in an ethylene glycol–water system boiling at 178 °C. The nanowires produced in this synthesis were highly monodispersed, with an average diameter of 98 ± 3 nm and average length of 1.80 ± 0.16 µm. (C, D) The TEM image and electron microdiffraction pattern obtained from an individual nanowire. Electron diffraction patterns taken from various sites of an individual nanowire indicates that nanowires synthesized using the present method were crystallized in a single crystalline trigonal phase with growth direction along the *c*-axis (as indicated by the arrow).

nearly monodispersed indicating homogeneous nucleation over a short period of time. These nanorods formed very quickly (within 1 min of mixing reagents) and showed very little change in the first hour after hydrazine had been added. This observation indicated that the initial growth was very fast and then slowed down markedly. These *t*-Te nanorods could exist as stable suspensions for a period of 1–3 days without adding any surfactant. If these unprotected nanorods were allowed to remain in solution longer than this period of time, they tended to form large aggregates and settle to the bottom of the container.

Reduction of tellurium dioxide by ethylene glycol

In addition to orthotelluric acid, we have also explored the use tellurium dioxide as a precursor to elemental tellurium. Due to the lower redox potential of Te(IV) relative to Te(VI), TeO_2 could be directly reduced by EG without adding hydrazine. Fig. 7 shows typical needle-shaped nanowires that were formed by reducing TeO_2 with EG at 180 °C. These nanostructures were very similar to the needle-shaped nanowires formed with the water–EG–hydrazine system, with rounded tips and uniform cross-sections (average width of 60 nm and average length on the order of tens of µm). Needle-shaped nanowires were the only product observed at temperatures above 180 °C.

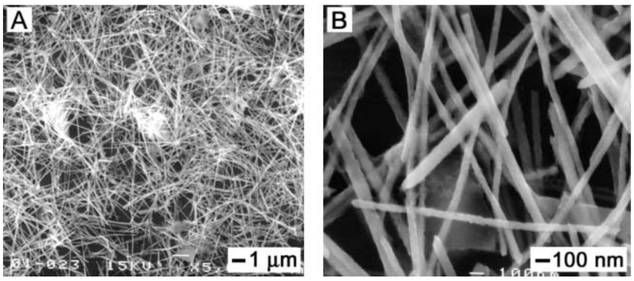

Fig. 7 (A) Low and (B) high magnification SEM images of *t*-Te nanowires that were synthesized by reducing tellurium dioxide with ethylene glycol at 180 °C. The shape of these nanowires is similar to that of n-whiskers having uniform hexagonal cross-sections and high aspect-ratios. The dimensions of the shown nanowires were polydisperse with an average width of 60 nm, and lengths on the order of tens of micrometers.

We believe that by fine-tuning the concentration of TeO_2 and the reaction temperatures, one can also attain good size control over these Te nanowires. A complete study of the reduction of tellurium dioxide by EG is beyond the scope of this work, and a more detailed analysis will soon follow.

Nucleation and growth mechanisms

We believe that the nucleation and growth of tellurium nanowires in pure water followed a mechanism similar to what we proposed for the formation of selenium nanowires. That is, the initial product of the reduction was a mixture of *a*-Te colloids and *t*-Te nanocrystallites. Because *t*-Te has a lower free energy relative to *a*-Te, the nanocrystallites could grow with a constant supply of ad-atoms that were readily available from the slow dissolution of *a*-Te colloids. This growth mechanism is consistent with what we observed over the course of reduction. Upon adding hydrazine to orthotelluric acid solution, the reaction mixture immediately changed its color from water white to cloudy black–brown, indicating the formation of a stable suspension of *a*-Te colloids.[17] Over the course of several hours, the brown suspension proceeded to form a silver–grey precipitate. The SEM images in Figs. 2C and 2D clearly show the presence of *a*-Te colloids that had not completely dissolved in the growth process. If this mixture of *a*-Te colloids and *t*-Te nanocrystallites was kept in the solution phase at room temperature for several months, the amorphous material would be completely transferred into the trigonal form.

The nucleation and growth of tellurium nanowires in ethylene glycol (and mixtures with water) seemed to follow a different mechanism. The only observed products of these reactions were *t*-Te nanostructures, and there was no evidence of *a*-Te colloids even at early sampling times. In the case of pure EG, the tellurium proceeded directly to the trigonal phase in the form of f-nanowires. It was likely that the higher temperature allowed for less restriction of the ad-atoms to rearrange into the more stable, trigonal form, rather than forming the amorphous phase seen in the pure water synthesis at temperatures < 100 °C.

We believe that the spine-like morphology was a result of trapped defects at the growing tips of s-nanowires. When the growth was carried out in water and at temperatures below 100 °C, the relatively low mobilities of trapped defects and ad-atoms could both lead to the deviations from morphologies with cross-sections that one would expect for a perfect hexagonal structure of trigonal Te. Raising the temperature would increase the mobility of Te in both solution and solid states, and facilitate the escape of crystal imperfections. That is why filamentary or needle-shaped nanowires with more symmetric cross-sections were obtained when the growth was performed at temperatures above 100 °C. The subtle difference between pure EG and mixtures of EG and water is yet to be completely understood. We believe that the filamentary morphology observed for the pure EG system was caused by the relatively low supersaturation at the growth tips. When EG was combined with a very small amount of water, the solubility of orthotelluric acid could be readily dissolved at room temperature. In addition, water should be a better medium for tellurium atoms to diffuse through than EG due to its relatively low viscosity. These two factors will ensure a high supersaturation of Te atoms at the growth tips, and allow us to obtain defect-free, n-nanowires having uniform hexagonal cross-sections.

In general, the tellurium nanostructures obtained through the solution-phase routes were single crystalline as verified by electron diffraction studies. Each sample was also analyzed by X-ray diffraction and displayed the characteristic peaks for the crystal planes of trigonal Te.[22] Fig. 8 shows a typical powder diffraction pattern taken from a sample prepared in pure water at room temperature. All of the diffraction peaks could be indexed to the trigonal phase of tellurium.

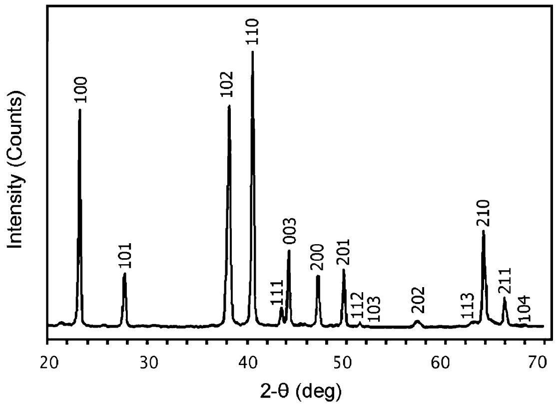

Fig. 8 The XRD pattern of tellurium nanowires synthesized by reducing orthotelluric acid with hydrazine in water (refluxed at 100 °C). All peaks in this pattern could be indexed to trigonal tellurium. Tellurium nanowires obtained under other conditions described in this paper also exhibited similar XRD patterns.

IV. Conclusions

We have demonstrated a simple, convenient and versatile route to the large-scale synthesis of single crystalline nanostructures of *t*-Te with a variety of morphologies. These nanostructures were characterized as high purity tellurium, crystallized in the trigonal lattice. As with other soft, solution-phase methods, the synthetic approach described here displays several advantages over gas-phase reactions, such as cost effectiveness, environmentally benign reaction conditions, and relatively low processing temperatures (< 200 °C). The solution-phase approach described in this paper also has a number of other attractive features: First, the reaction does not require a substrate or any heterogeneous nucleation source to produce a wide variety of 1D nanostructures. This allows for freestanding nanostructures with the potential for larger scale synthesis than conventional methods. All of these nanostructures are free of unwanted heterogeneous domains made of other materials. Second, the anisotropic crystal structure of tellurium provides a natural template that defines and directs the growth of these nanostructures. In the case of the n- and s-whiskers, growth is largely confined to the *c*-axis allowing for nanostructures with very high aspect ratios. Third, the reaction involved is intrinsically clean, yielding only tellurium metal, nitrogen gas, and water. Fourth, scale-up of this reaction for large-scale synthesis of nanomaterials is relatively simple because it can be carried out in solution at ambient pressure. In addition, the single crystalline nanostructures described in this paper were demonstrated to be quite stable. Samples were found to be well-preserved with almost no physical degradation for periods greater than one year, when stored in darkness.

Acknowledgement

This work has been supported in part by a Career Award from the NSF (DMR-9983893), an AFOSR-DURINT subcontract from SUNY-Buffalo, and a Research Fellowship from the David and Lucile Packard Foundation. Y.X. is an Alfred P. Sloan Research Fellow (2000–2002). B.M. thanks the Center for Nanotechnology at the UW for an IGERT Fellowship Award funded by the NSF (DGE-9987620).

References

1 (*a*) H. M. Huang, S. Mao, H. Feick, H. Yan, Y. Wu, H. Kind, E. Weber, R. Russo and P. Yang, *Science*, 2001, **292**, 1897;

(*b*) X. Duan, Y. Huang, Y. Cui, J. Wang and C. M. Lieber, *Nature*, 2001, **409**, 66; (*c*) S.-W. Chung, J.-Y. Yu and J. R. Heath, *Appl. Phys. Lett.*, 2000, **76**, 2068; (*d*) S. Frank, P. Poncharal, Z. L. Wang and W. A. de Heer, *Science*, 1998, **280**, 1744.

2 (*a*) S. Link, C. Burda, M. B. Mohamed, B. Nikoobakht and M. A. El-Sayed, *Phys. Rev. B*, 2000, **61**, 6068; (*b*) Z. L. Wang, *Adv. Mater.*, 2000, **12**, 1295; (*c*) J. Hu, T. W. Odom and C. M. Lieber, *Acc. Chem. Res.*, 1999, **32**, 435; (*d*) S. M. Prokes and K. L. Wang, *MRS Bull.*, 1999, **24**(8), 13; (*e*) L. Brus, *J. Phys. Chem.*, 1994, **98**, 3575; (*f*) A. D. Alivisatos, *MRS Bull.*, 1995, August, 23.

3 Y. Xia, J. A. Rogers, K. Paul and G. M. Whitesides, *Chem. Rev.*, 1999, **99**, 1823.

4 (*a*) G. A. Ozin, *Adv. Mater.*, 1992, **4**, 612; (*b*) H. Weller, *Angew. Chem., Int. Ed. Engl.*, 1993, **32**, 41; (*c*) J. H. Fendler, *Chem. Rev.*, 1987, **87**, 877.

5 (*a*) A. P. Alivisatos, *Science*, 1996, **271**, 933; (*b*) E. Matijevic, *Chem. Mater.*, 1993, **5**, 412.

6 See, for example: (*a*) J. M. Schnur, *Science*, 1993, **262**, 1669; (*b*) C. R. Martin, *Science*, 1994, **266**, 1961; (*c*) S. C. Tsang, Y. K. Chen, P. J. F. Harris and M. L. H. Green, *Nature*, 1994, **372**, 159; (*d*) H. Dai, E. W. Wong, Y. Z. Lu, S. Fan and C. M. Lieber, *Nature*, 1995, **375**, 769; (*e*) B. R. Martin, D. J. Dermody, B. D. Reiss, M. M. Fang, L. A. Lyon, M. J. Natan and T. E. Mallouk, *Adv.Mater.*, 1999, **11**, 1021.

7 E. I. Givargizov, *Highly Anisotropic Crystals*, ed. I. Sunagawa, D. Reidel Publishing Company, Boston, MA, 1987.

8 (*a*) N. G. Chopra, R. J. Luyken, K. Cherrey, V. H. Crespi, M. L. Cohen, S. G. Louie and A. Zettl, *Science*, 1995, **269**, 966; (*b*) J. Kong, H. T. Soh, A. M. Cassell, C. F. Quate and H. Dai, *Nature*, 1998, **385**, 878.

9 (*a*) X. Duan and C. M. Lieber, *Adv. Mater.*, 2000, **12**, 298; (*b*) S. T. Lee, N. Wang, Y. F. Zhang and Y. H. Tang, *MRS Bull.*, 1999, **24**(8), 36; (*c*) Y. Y. Wu and P. D. Yang, *Chem. Mater.*, 2000, **12**, 605; (*d*) Z. W. Pan, Z. R. Dai and Z. L. Wang, *Science*, 2001, **291**, 1947; (*e*) W. Shi, Y. Zheng, N. Wang, C.-S. Lee and S.-T. Lee, *Adv. Mater.*, 2001, **13**, 591.

10 (*a*) M. Yazawa, M. Koguchi, A. Muto and K. Hiruma, *Adv. Mater.*, 1993, **5**, 577; (*b*) R. S. Wagner and W. C. Ellis, *Appl. Phys. Lett.*, 1964, **4**, 89; (*c*) E. I. Givargizov, *J. Vac. Sci. Technol. B*, 1993, **11**, 449; (*d*) N. Ozaki, Y. Ohno and S. Takeda, *Appl. Phys. Lett.*, 1998, **73**, 3700.

11 (*a*) T. J. Trentler, K. M. Hickman, S. C. Goel, A. M. Viano, P. C. Gibbons and W. E. Buhro, *Science*, 1995, **270**, 1791–1794; (*b*) Y. Xie, P. Yang, J. Lu, W. Wang and Y. Qian, *Chem. Mater.*, 1999, **11**, 2619–2622; (*c*) J. D. Holmes, K. P. Johnston, R. C. Doty and B. A. Korgel, *Science*, 2000, **287**, 1471–1473.

12 (*a*) *Tellurium*, Ed. W. C. Cooper, Van Nostrand Reinhold Co., New York, 1971; (*b*) L. I. Berger, *Semiconductor Materials*; CRC Press, Boca Raton, FL, 1997, pp. 86–88.

13 (*a*) A. A. Kudryavtsev, *The Chemistry and Technology of Selenium and Tellurium*, Collet's, (Publishers)Ltd., London, 1974; (*b*) T. Ikari, H. Berger and F. Levy, *Mater. Res. Bull.*, 1986, **21**, 99; (*c*) K. Araki and T. Tanaka, *Jpn. J. Appl. Phys.*, 1972, **11**, 472; (*d*) V. B. Ufimtsev, V. B. Osvensky, V. T. Bublik, T. B. Sagalova and O. E. Jouravlev, *Adv. Perf. Mater.*, 1997, **4**, 189.

14 G. Henshaw, I. P. Parkin and G. A. Shaw, *J. Chem. Soc., Dalton Trans.*, 1997, 231–236.

15 (*a*) B. Gates, B. Mayers, B. Cattle and Y. Xia, *Adv. Funct. Mater*, 2002, **12**, 219–227; (*b*) B. Gates, Y. Yin and Y. Xia, *J. Am. Chem. Soc.*, 2000, **122**, 12582.

16 (*a*) N. Furuta, Y. Ohasi, H. Itinose and Y. Igarashi, *Jpn. J. Appl. Phys.*, 1975, **14**, 929; (*b*) N. Furuta, H. Itinose, N. Maruyama and Y. Ohasi, *Jpn. J. Appl. Phys.*, 1972, **11**, 1113.

17 (*a*) A.-M. Joseph-Petit, F. Dumont and A. Watillon, *J. Colloid Interface Sci.*, 1973, **43**, 649; (*b*) T. W. Smith and R. A. Cheatham, *Macromolecules*, 1980, **13**, 1203; (*c*) Y. Zhu, Y. Qian, H. Huang and M. Zhang, *Mater. Lett.*, 1996, **28**, 119; (*d*) J. A. Johnson, M.-L. Saboungi, R. Csensits and D. Meisel, *J. Phys. Chem. B*, 1999, **103**, 59.

18 (*a*) E. Grison, *J. Chem. Phys.*, 1951, **19**, 109; (*b*) D. Quere, J.-M. Di Meglio and F. Brochard-Wyart, *Science*, 1990, **249**, 1256.

19 (*a*) *Glycols*, eds. G. O. Cume and F. Johnston, Reinhold Publishing Co., New York, 1952; (*b*) D. R. Corday, L. R. Kaplan, P. M. Woyciesjes and T. F. Kozak, *Fluid Phase Equilib.*, 1996, **117**, 146.

20 (*a*) F. Fievet, J. P. Lagier and M. Figlarz, *MRS Bull.*, 1989, December, 29; (*b*) F. Fievet, F. Fievet-Vincent, J. Lagier, B. Dumont and M. Figlarz, *J. Mater. Chem.*, 1993, **3**, 627.

21 B. Mayers and Y. Xia, *Adv. Mater.*, 2002, **14**, 279–282.

22 P. Unger and P. Cherin, in *The Physics of Selenium and Tellurium*; Pergamon Press, New York, NY, 1969, pp. 223–229.